Journal of Computational Physics 228 (2009) 4491–4509

Contents lists available at ScienceDirect

Journal of Computational Physics

journal homepage: www.elsevier.com/locate/jcp

The piecewise-linear Finite Volume scheme: The best known lowest-order preconditioner for the $\frac{d^2}{dx^2}$ Chebyshev spectral operator

G. Labrosse *

Université Paris-sud, Limsi-CNRS, BP 133, 91403 Orsay Cedex, France

ARTICLE INFO

Article history:
Received 15 September 2008
Received in revised form 5 March 2009
Accepted 16 March 2009
Available online 25 March 2009

Keywords:
Spectral Chebyshev approximation
Preconditioning
Finite Difference method
Finite Element method
Finite Volume method

ABSTRACT

The low-order (3-node) Finite Volume (FV) preconditioning technique is considered for its efficiency to spectrally solve the $\mathcal{L}[u] \equiv \frac{d^2y}{dx^2} = f$ problem. The Fourier spectrum of the associated preconditioning operator is analytically determined and compared with the known Fourier spectra of the corresponding Finite Difference (FD) and Finite Element (FE) preconditioning operators. Moreover, following what was done in [P. Haldenwang, G. Labrosse, S. Abboudi, M.O. Deville, Chebyshev 3-d spectral and 2-d pseudospectral solvers for the Helmholtz equation, J. Comput. Phys. 55 (1984) 115–128] for the FD case, the FE and FV preconditioning operator Chebyshev spectra are analytically determined, first without reference to boundary conditions, and then confirmed when Dirichlet boundary conditions are imposed. The convergence of the Chebyshev towards the Fourier spectra is established. All this analysis leads to conclude that the best of the known lowest-order preconditioners is provided by the piecewise-linear Finite Volume scheme.

1. Introduction

Accurate numerical experiments bring valuable contributions to the understanding of confined flow dynamics. The accurate determination of the Stokes eigenmodes, [16,17], or the DNS validation of turbulence models, [15], is convincing illustrations. For these cases, minimizing the numerical biases is more than recommendable since they are recycled by the flow itself. In this respect, spectral methods are well recognized for their ability to supply physically relevant numerical incompressible flows, with accurate determination of transition thresholds, bifurcation diagrams and statistical correlations. However their use is limited to configurations where the boundary conditions are imposed on orthogonal geometries. This is a major restriction. Indeed, confined flow dynamics is very sensitive to the shape of the boundaries [3], and moreover, in a number of cases, a free surface is involved and interacts with the fluid flow, or even generates it.

Among the configurations which cannot be modeled with orthogonal geometries, there are many of them, natural or industrial, which do not require a complex-geometry approach with its multi-domain option. In these situations, a spectrally accurate mono-domain treatment of the Navier–Stokes equations can be designed, and implemented, in such a way that the resulting numerical complexity and computational cost are not much larger than those coming from orthogonal geometries [3]. The way was opened up in [19]: given N a cut-off frequency, it was proposed that the desired spectral solution $u_N(x)$ of the linear problem $\mathcal{L}[u(x)] = f(x)$ be obtained from a finite precision operator, $\mathcal{L}_{app}$, instead of $\mathcal{L}$. This is carried out iteratively. An initial guess $u_N^{(0)}(x)$, obtained for instance from $\mathcal{L}_{app}[u_N^{(0)}(x)] = f_N(x)$, is successively corrected, $u_N^{(1)}(x) = u_N^{(0)}(x) + \alpha(\delta u_N^{(0)}(x))$, and so on, by a sequence of $(\delta u_N^{(n)}(x))$'s verifying $\mathcal{L}_{app}[\delta u_N^{(n)}(x)] = f_N(x) - \mathcal{L}[u_N^{(n)}(x)]$, $f_N(x)$ being the polynomial which approximates $f(x)$. The efficiency of this method (or, for that matter, of any other iterative method) depends on the choice of $\mathcal{L}_{app}$: it should lead to an easily invertible matrix and be as close as possible to $\mathcal{L}$. The closer the condition number of the matrix

* Tel.: +33 169858072; fax: +33 169858088.
E-mail address: gerard.labrosse@u-psud.fr

0021-9991/$ - see front matter © 2009 Elsevier Inc. All rights reserved.
doi:10.1016/j.jcp.2009.03.019

representing $\mathcal{L}_{app}^{-1}\mathcal{L}$ is to *1*, the more efficient is the method and the closer to 1 is α, the relaxation parameter. Since then, both FD [12–14] and FE [2,7,4,10,8] preconditioners have been considered and Fourier analyzed, the latter one being significantly better than the former. FE preconditioning has been used for solving the linearized Navier–Stokes problem, with a multi-domain strategy, and applied to test problems like the regularized driven square cavity and the backward facing step [5], and also to thermal problems [6].

Knowing that the ultimate goal is, of course, to solve 2D/3D elliptic differential equations, it is advisable to identify the best $\frac{d^2}{dx^2}$ preconditioner of lowest order, that is based on a *3*-node local approximation of $\frac{d^2}{dx^2}$.

The present paper reports on Fourier and Chebyshev theoretical analyses of all the *3*-node FD, FE and FV preconditionings that can be designed for the $\mathcal{L}[u] \equiv \frac{d^2u}{dx^2}$ problem. In particular the exact eigenvalues of the Chebyshev matrices representing $\mathcal{L}_{app}^{-1}\mathcal{L}$ are presented. They are obtained by applying the procedure developed in [12], that is without taking boundary conditions into account. This completes the work presented in [10] where only approximate eigenvalues are quoted for the FE preconditioning. It is then shown that the eigenvalues so obtained are not modified when Dirichlet boundary conditions are imposed. All that leads to a conclusion: among the FD, FE and FV *3*-node preconditioners, the piecewise-linear FV approximation provides the best *3*-node preconditioning of the $\frac{d^2}{dx^2}$ Chebyshev spectral operator.

The analysis is carried out taking as a guide the elliptic eigenvalue problem whose differential part reads

$$\mathcal{L}[u(x)] \equiv \frac{d^2u}{dx^2} = \xi u(x), \quad \text{for } x \in]-1,1[\text{ and } \xi < 0. \tag{1}$$

Let $\mathbb{P}_N$ be the space of polynomials of highest degree N, the integer N being also the number of intervals (defined at the discretization stage) covering

$$\mathcal{I} = [-1,1]. \tag{2}$$

Any numerical approximation $u_N(x)$ of $u(x)$ lies in $\mathbb{P}_N$ and can therefore be treated as a continuous function. This allows us to give the spectral and local approximations of (1) the following writing

$$\mathcal{L}_{sp}[u_N(x)] = \xi_{sp}u_N(x), \quad \mathcal{L}_{app}[u_N(x)] = \xi_{app}u_N(x), \quad \text{for } x \in]-1,1[.$$

In the discrete realm, $\mathcal{L}_{sp}$ and $\mathcal{L}_{app}$ are represented by square matrices, of size $(N+1)$, usually of two kinds. Constructed in physical space, then called collocation matrices, they are denoted by L_{sp} and L_{app}, respectively. They can also be defined in pseudo-spectral space, then noted $\widehat{L}_{sp}$ and $\widehat{L}_{app}$. Then, for the preconditioning operator $\mathcal{L}_{app}^{-1}\mathcal{L}_{sp}$, one deals with either a collocation ($L_{app}^{-1}L_{sp}$) or a pseudo-spectral ($\widehat{L}_{app}^{-1}\widehat{L}_{sp}$) matrix. Since the L and $\widehat{L}$ matrices are in similitude relationship, the matrices $L_{app}^{-1}L_{sp}$ and $\widehat{L}_{app}^{-1}\widehat{L}_{sp}$ have identical eigenvalues. It turns out that the analytical treatment can be completely worked out in pseudo-spectral space, i.e. with $\widehat{L}_{app}^{-1}\widehat{L}_{sp}$.

When the discretization is based on regular grids, it is well known [22] that the Fourier functions are eigenmodes of the matrices. The eigenvalues ξ_{sp} and ξ_{app} are then very easy to express, and the $L_{app}^{-1}L_{sp}$ spectrum can be straightforwardly written as

$$\xi\left[L_{app}^{-1}L_{sp}\right] = \frac{\xi_{sp}}{\xi_{app}}.$$

Conversely, performing the Chebyshev analysis is significantly more involved.

- In a first step the problem (1) is discretized without adding any boundary condition. In this polynomial approach, the eigenvalues of L_{sp} and L_{app} are all zero. But, once the matrix $\widehat{L}_{app}^{-1}$ is properly defined, the $L_{app}^{-1}L_{sp}$ eigenvalues no longer cancel. The structure of the $\widehat{L}_{sp}$ and $\widehat{L}_{app}$ matrices can be anticipated from basic arguments. They lead to $\widehat{L}_{app}^{-1}\widehat{L}_{sp}$ matrices which are upper triangular. The analytical writing of the $\widehat{L}_{app}^{-1}\widehat{L}_{sp}$ eigenvalues is therefore straightforward if the $\widehat{L}_{app}$ entries can themselves be analytically expressed. This is a significant part of the work.
- In a second step, it is shown that imposing Dirichlet boundary conditions does not modify the previously determined $L_{app}^{-1}L_{sp}$ eigenvalues.

The paper contains two main sections and two appendices. Sections 2 and 3 present analyses of the FD, FE and FV *3*-node preconditioners of $\frac{d^2}{dx^2}$, successively the Fourier analysis for the approximations based on uniform meshes, and the Chebyshev analysis for a Gauss–Lobatto (and hence, non uniform) mesh. Appendix A is just a reminder of the FV approach. The detailed analytical determination of the $L_{app}^{-1}L_{sp}$ Chebyshev eigenvalues is deferred to Appendix B.

In order to make this paper as short as possible, the required theoretical background is assumed to be known, and can be found in the monograph [11] and the textbook [1].

2. Fourier analysis

2.1. Foreword

Although the goal is to discretize $\frac{d^2}{dx^2}$ on a Chebyshev Gauss–Lobatto grid, it is useful to Fourier analyze the $L_{app}^{-1}L_{sp}$ matrices. This amounts to discretizing with regular grids, then leading to Toeplitz matrices [22] whose eigenmodes are the complex

Fourier functions. The spectra are thus straightforwardly expressed, and have the virtue of being directly usable as a fairly good estimate of the $L_{app}^{-1}L_{sp}$ Chebyshev spectrum, as well known from [12], and confirmed here on a more general basis.

2.2. Trigonometric expansion and associated grids

The Fourier functional basis defined on $\mathcal{I}$, (2), is the set $\{e^{in\pi x}, n = -N,\ldots,N-1\}$, the corresponding grid being made of $2N$ equispaced nodes of coordinates $\{x_p = \frac{p}{N}, p = -N,\ldots,N-1\}$. The mesh size is

$$h \equiv \Delta x = \frac{1}{N}.$$

By periodicity, the node at $x = 1$ is absent from the data. The trigonometric approximation $u_N(x)$ of any $u(x)$ function is written as

$$u_N(x) = \sum_{n=-N}^{N-1} \widehat{u}_n e^{in\pi x},$$

where the set $\{\widehat{u}_n, n = -N,\ldots,N-1\}$ is the pseudo-spectrum. Determined so that

$$u_N(x_p) = u(x_p), \quad p = -N,\ldots,N-1,$$

be verified, it reads

$$\widehat{u}_n = \frac{1}{2N}\sum_{p=-N}^{N-1} e^{-inp\frac{\pi}{N}} u(x_p), \quad n = -N,\ldots,N-1.$$

The following notation is adopted in the sequel of this section and whenever one deals with a periodic approximation,

$$u_p \equiv u_N(x_p), \quad p = -N,\ldots,N-1,$$

together with the column vector

$$U = (u_p, p = -N,\ldots,N-1)^t.$$

2.3. 3-Node local approximations

Our schemes are denoted by FD2, FE1, FV1 and FV2. The FD2 scheme is of second order in h, based on centered differences (see [18] for example). The FE1 scheme (see [21] for example) and FV1 scheme (see [9] for example, and Section A.1 of Appendix A) are designed from a piecewise-linear approximation of $u(x)$ over each of the $(2N-1)$ intervals $x \in [x_p, x_{p+1}]$, $p = -N,\ldots,N-2$. The FV2 scheme (see Section A.2 of Appendix A) uses a piecewise-quadratic approximation of $u(x)$ over each of the $(2N-1)$ intervals $x \in [x_{p-1}, x_{p+1}]$, $|p| = 0,\ldots,N-1$, while imposing $u_N = u_{-N}$. A second grid is needed for the FV approach. It is made of $(2N-1)$ midpoints of coordinates

$$\chi_p = x_{p-\frac{1}{2}} \equiv x_p - \frac{h}{2}, \quad |p| = 0,\ldots,N-1.$$

The FV formulation therefore involves the nodal values $u_N(\chi_p)$ together with the unknown u_p's. The $u_N(\chi_p)$'s are eliminated in terms of the u_p's using the relation (41) for the piecewise-linear approximation, and (43) for the piecewise-quadratic approximation.

The generic notation L_{app} is here updated according to $L_{app} \Rightarrow L^{(\bullet)}$, together with $\xi_{app} \Rightarrow \xi^{(\bullet)}$, where $\bullet$ stands for FD2, FE1, FV1 or FV2. Both FE and FV formulations of $\mathcal{L}[u(x)] = \xi u(x)$ lead to a stiffness and mass factorization of L_{app} having the general form

$$L_S^{(\bullet)}U = \xi^{(\bullet)} L_M^{(\bullet)}U, \quad \bullet = FE1, FV1, FV2.$$

The discrete systems are now successively written. For FD2, one simply has

$$(L^{(FD2)}U)_p \equiv \frac{1}{h^2}[u_{p-1} - 2u_p + u_{p+1}] = \xi^{(FD2)}u_p, \quad p = -N,\ldots,N-1.$$

For FE1, FV1 and FV2, still for $p = -N,\ldots,N-1$, they read

$$\left(L_S^{(\bullet)}U\right)_p = \xi^{(\bullet)}\left(L_M^{(\bullet)}U\right)_p, \quad \bullet = FE1, FV1, FV2,$$

where

$$\left(L_S^{(FE1)}U\right)_p = \left(L_S^{(FV1)}U\right)_p = \left(L_S^{(FV2)}U\right)_p = \frac{1}{h}[u_{p-1} - 2u_p + u_{p+1}], \tag{3}$$

and

$$\begin{aligned}\left(L_M^{(FE1)}U\right)_p &= \frac{h}{6}\left[u_{p-1}+4u_p+u_{p+1}\right],\\ \left(L_M^{(FV1)}U\right)_p &= \frac{h}{8}\left[u_{p-1}+6u_p+u_{p+1}\right],\\ \left(L_M^{(FV2)}U\right)_p &= \frac{h}{24}\left[u_{p-1}+22u_p+u_{p+1}\right].\end{aligned} \tag{4}$$

Being of Toeplitz type [22], these systems have the $\{e^{in\pi x}, |n| = 0,\ldots,N\}$ as eigenmodes. Their eigenvalues are thus easily written down.

2.4. $L_{app}^{-1}L_{sp}$ Fourier eigenvalues

The eigenvalues $\xi[L_{app}^{-1}L_{sp}]$ simply read

$$\xi\left[L_{app}^{-1}L_{sp}\right] = \frac{\xi_{sp}}{\xi_{app}}, \quad \xi_{sp} = \{-n^2\pi^2, |n| = 0,\ldots,N\}.$$

One gets

$$\xi_n\left[\left(L^{(FD2)}\right)^{-1}L_{sp}\right] = \left(\frac{n\pi\frac{h}{2}}{\sin\left(n\pi\frac{h}{2}\right)}\right)^2, \quad |n| = 0,\ldots,N, \tag{5}$$

$$\xi_n\left[\left(L^{(FE1)}\right)^{-1}L_{sp}\right] = \xi_n\left[\left(L^{(FD2)}\right)^{-1}L_{sp}\right]\frac{1+2\cos^2\left(n\pi\frac{h}{2}\right)}{3}, \quad |n| = 0,\ldots,N, \tag{6}$$

$$\xi_n\left[\left(L^{(FV1)}\right)^{-1}L_{sp}\right] = \xi_n\left[\left(L^{(FD2)}\right)^{-1}L_{sp}\right]\frac{1+\cos^2\left(n\pi\frac{h}{2}\right)}{2}, \quad |n| = 0,\ldots,N, \tag{7}$$

$$\xi_n\left[\left(L^{(FV2)}\right)^{-1}L_{sp}\right] = \xi_n\left[\left(L^{(FD2)}\right)^{-1}L_{sp}\right]\frac{5+\cos^2\left(n\pi\frac{h}{2}\right)}{6}, \quad |n| = 0,\ldots,N.$$

The $L_{app}^{-1}L_{sp}$ spectral radius is

$$r = \frac{M-m}{M+m},$$

where m and M are, respectively, the smallest and largest values of $\xi_n[L_{app}^{-1}L_{sp}]$. The smaller the value of r, the closer $\mathcal{L}_{app}$ is to $\mathcal{L}_{sp}$.

One gets

$$r(FD2, FE1, FV1, FV2) = (0.42, 0.18, 0.15, 0.35). \tag{8}$$

The FV1 scheme is thus the best 3-node preconditioner of the $\frac{d^2}{dx^2}$ Fourier solver. This conclusion is illustrated in Fig. 1 which shows the spectra $\xi_n\left[L_{app}^{-1}, L_{sp}\right]$ as functions of nh, taken as continuous in $[0,1]$ for $|n| \in [0,N]$. The FD2 and FV2 schemes are clearly low-pass filters. They underestimate, in a monotonic way, the $\frac{d^2}{dx^2}$ effect, more and more as the spatial frequency increases, for $\eta \in]0,1]$, that is from $|n| = 1$ until $|n| = N$. The FE1 and FV1 curves are similar, but only FV1 presents compensation effects between low and high frequencies, around $nh = 0.86$, where $\xi_n\left[L_{app}^{-1}L_{sp}\right] = 1$. It indeed overestimates the second derivative of the low-frequency components, for $1 < |n| < 0.86N$, and underestimates the second derivative of the remaining high frequency components.

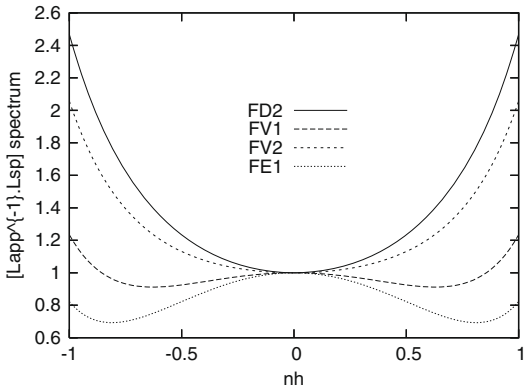

Fig. 1. $L_{app}^{-1}L_{sp}$ Fourier eigenvalues for the 3-node approximations.

3. Chebyshev analysis

3.1. Foreword

Obtaining the Chebyshev version of the $L_{app}^{-1}L_{sp}$ Fourier eigenvalues listed in Section 2.4 is very much more laborious. The first Chebyshev analysis of a local-approximation preconditioner, the FD2 scheme, was published in [12]. The trigonometric nature of the Chebyshev polynomials is the key for working out an analytical description of the $\widehat{L}_{app}$ matrix. It is also observed in [12] that the Chebyshev $L_{app}^{-1}L_{sp}$ eigenvalues are real, and converge with N towards the Fourier eigenvalues (5). We will see below that this holds also for FE1 and FV1. An attempt at applying the method given in [12] to the FE1 case came later [10]. It led to complex $L_{app}^{-1}L_{sp}$ eigenvalues. The reason for this result is due to the way that the analysis was conducted (see Sections 3.3.1 and A.3). The FV2 scheme is discarded, since the Fourier analysis does not give it interesting prospects. This section is therefore dedicated to the treatment of the nodal equations,

$$\left(L^{(FD2)}U\right)_p = \xi^{(FD2)}u_N(x_p), \quad p = 1,\ldots,N-1, \tag{9}$$

and

$$\left(L_S^{(\bullet)}U\right)_p = \xi^{(\bullet)}\left(L_M^{(\bullet)}U\right)_p, \quad p = 1,\ldots,N-1;\ \bullet = FE1, FV1, \tag{10}$$

where

$$U = \left(u_N(x_p), p = 0,\ldots,N\right)^t. \tag{11}$$

The left- and right-hand side terms are evaluated at the internal Chebyshev Gauss–Lobatto nodes (Section 3.2). In a first step, without any boundary condition, the relations (9) and (10) are used for writing down the $(N+1)^2$ entries of the $\widehat{L}_{app}$ matrices. This leads to the $L_{app}^{-1}L_{sp}$ eigenvalues analytical expression, together with their connection with the corresponding Fourier eigenvalues. Finally, a simple argument is given showing that imposing Dirichlet boundary conditions does not modify these eigenvalues.

3.2. Chebyshev expansion and associated grids

A functional basis of $\mathbb{P}_N$ can be constructed over the interval $\mathcal{I}$, (2), with the set of Chebyshev polynomials in $x = -\cos(\theta)$, $\{T_n(x) = (-1)^n\cos(n\theta),\ n = 0,\ldots,N\}$. The grid is made of $(N+1)$ *Gauss–Lobatto* nodes whose coordinates are

$$x_p = -\cos(\theta_p), \quad \theta_p = p\frac{\pi}{N};\ p = 0,\ldots,N.$$

The mesh sizes are denoted by

$$h_p = x_p - x_{p-1}, \quad p = 1,\ldots,N.$$

The *Gauss* nodes are taken as FV1 intermediate nodes (Section A.1 in Appendix A). Their coordinates are (see Fig. 2 for $N = 6$),

$$\chi_p = -\cos\left(\frac{(2p-1)\pi}{2N}\right) = -\cos\left(\theta_p - \frac{\pi}{2N}\right), \quad p = 1,\ldots,N. \tag{12}$$

The polynomial approximation $u_N(x)$ of any function $u(x)$ is written as

$$u_N(x) = \sum_{n=0}^{N}\widehat{u}_n T_n(x), \tag{13}$$

where the pseudo-spectrum $\{\widehat{u}_n, n = 0,\ldots,N\}$ is determined so that

$$u_N(x_p) = u(x_p), \quad p = 0,\ldots,N.$$

It reads

$$\widehat{u}_n = \frac{2}{N\bar{c}_n}\sum_{p=0}^{N}\frac{1}{\bar{c}_p}T_n(x_p)u(x_p), \quad n = 0,\ldots,N, \tag{14}$$

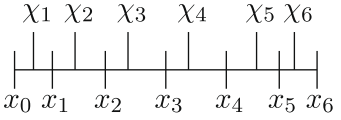

Fig. 2. FV1 double grid for $N = 6$.

with

$$\bar{c}_0 = \bar{c}_N = 2, \quad \bar{c}_n = 1 \quad \text{for } 1 \leqslant n \leqslant N-1.$$

The following notation is adopted in the sequel of this Section and whenever one deals with the polynomial approximation,

$$u_p \equiv u_N(x_p), \quad p = 0, \ldots, N.$$

Let us give both relations, (13) evaluated at all the x_p's, and (14), a matrix form by introducing, beside U given by (11), a second column vector,

$$\widehat{U} = \left(\widehat{u}_n, \quad n = 0, \ldots, N\right)^t,$$

and the $\mathcal{T}$ matrix, together with its inverse, $\mathcal{T}^{-1}$, whose entries are

$$\mathcal{T}_{mn} = (-1)^n \cos\left(mn\frac{\pi}{N}\right), \quad \left(\mathcal{T}^{-1}\right)_{mn} = \frac{2(-1)^m}{N\bar{c}_m\bar{c}_n}\cos\left(mn\frac{\pi}{N}\right), \quad m,n = 0,\ldots,N. \tag{15}$$

One then has

$$U = \mathcal{T}\widehat{U}, \quad \widehat{U} = \mathcal{T}^{-1}U, \tag{16}$$

a relation pointing out the similitude which links the nodal value set and the pseudo-spectrum of any polynomial lying in $\mathbb{P}_N$.

3.3. Determination of the L_{app} and $\widehat{L}_{app}$ matrices

Let $\mathcal{L}$ be any operator acting from $\mathbb{P}_N$ to $\mathbb{P}_N$, that is such that $u_N^{(\mathcal{L})}(x) \equiv \mathcal{L}[u_N(x)]$ lies in $\mathbb{P}_N$. Two column vectors are introduced. The first one gathers the $u_N^{(\mathcal{L})}(x)$ nodal values,

$$U^{(\mathcal{L})} = \left(u_p^{(\mathcal{L})} \equiv u_N^{(\mathcal{L})}(x_p), p = 0, \ldots, N\right)^t = LU.$$

Then we construct the column vector of the $u_N^{(\mathcal{L})}(x)$ pseudo-spectrum,

$$\widehat{U}^{(\mathcal{L})} = \left(\widehat{u}_n^{(\mathcal{L})}, n = 0, \ldots, N\right)^t = \widehat{L}\widehat{U}.$$

The L and $\widehat{L}$ matrices are related by

$$L = \mathcal{T} \cdot \widehat{L} \cdot \mathcal{T}^{-1}.$$

Regarding the Chebyshev second derivative, L and $\widehat{L}$ are known as being respectively $L_{sp} \equiv D_T^2$ and $\widehat{L}_{sp} \equiv \widehat{D}_T^2$ (see Section 3.4.1). Here is presented the way the matrices L_{app} and $\widehat{L}_{app}$ can be expressed from stiffness and mass matrices defined only by the internal nodal values $(L_\bullet U)_p$, $p = 1, \ldots, N-1$ (see the discrete relations (32)–(35)).

3.3.1. The stiffness and mass square matrices, $\widehat{\mathbb{L}}_\bullet$ and $\mathbb{L}_\bullet$

Let us adopt a common writing (see Section 3.7) of the FD2, FE1 and FV1 schemes, viz.

$$(L_S U)_p = \xi_{app}(L_M U)_p, \quad p = 1, \ldots, N-1. \tag{17}$$

Using the first relation of (16) one can modify (17) as

$$(L_S\mathcal{T}\widehat{U})_p = \xi_{app}(L_M\mathcal{T}\widehat{U})_p, \quad p = 1, \ldots, N-1.$$

The analytical work presented in Appendix B shows that the rectangular matrices $L_S\mathcal{T}$ and $L_M\mathcal{T}$ can be factorized as

$$(L_\bullet\mathcal{T})_{pn} = \sqrt{1-x_p^2}(\mathcal{T}\widehat{\mathbb{L}}_\bullet)_{pn}, \quad \bullet = S, M, \quad \begin{cases} n = 0, \ldots, N, \\ p = 1, \ldots, N-1, \end{cases} \tag{18}$$

where the $\widehat{\mathbb{L}}_\bullet$'s are square matrices of size $(N+1)$.

3.3.2. The L_{app} and $\widehat{L}_{app}$ matrices

The $\widehat{\mathbb{L}}_M$ matrices are not of differential nature. They are therefore invertible, which leads directly to the factorization relation

$$\widehat{L}_{app} = \widehat{\mathbb{L}}_M^{-1} \cdot \widehat{\mathbb{L}}_S, \tag{19}$$

with also

$$L_{app} = \mathcal{T} \cdot \widehat{L}_{app} \cdot \mathcal{T}^{-1}. \tag{20}$$

3.3.3. An interesting by-product

An interesting by-product deserves to be mentioned. It regards the collocation matrices $L^{(\bullet)}$, with $\bullet$ = FD2, FE1 and FV1 (see Sections B.3, B.4.2 and B.5.2). They are square matrices of size $(N+1)$. The internal part of $L^{(FD2)}$ is, as expected, tridiagonal (see (51)), whereas the $L^{(FE1)}$ and $L^{(FV1)}$ matrices are full (see (55) and (62)). All these matrices supply an evaluation of the second derivative at all the nodes, including at the boundary nodes, $\left.\frac{d^2u_N}{dx^2}\right|_{0,N}$, with the accuracy of the corresponding scheme. These quantities $\left.\frac{d^2u_N}{dx^2}\right|_{0,N}$ are of global nature, even for FD2: they involve all the nodal values of $u_N(x)$. But, of course, the extreme rows of these L_{app} matrices are linear combination of the internal rows: they have to be replaced by the boundary conditions for the resulting matrix to be invertible.

3.4. Derivative operators

3.4.1. Chebyshev derivative operators

From the usual notation

$$u_N^{(2)}(x) \equiv \frac{d^2u_N(x)}{dx^2} = \sum_{n=0}^{N} \widehat{u}_n^{(2)} T_n(x)$$

one defines the column vector

$$\widehat{U}^{(2)} = \left(\widehat{u}_n^{(2)}, n = 0, \ldots, N\right)^t.$$

It is given by

$$\widehat{U}^{(2)} = \widehat{L}_{sp}\widehat{U} \equiv \widehat{D}_T^2\widehat{U},$$

where $\widehat{D}_T$ is the well known pseudo-spectral first-derivative matrix whose non-zero entries are

$$(\widehat{D}_T)_{nv} = \frac{2v}{c_n}; \quad v = 1, \ldots, N, \ n = v-1, v-3, \ldots, Mod[v-1, 2].$$

Here is an example of $\widehat{D}_T$ and $\widehat{D}_T^2$, written for $N = 5$,

$$\widehat{D}_T = \begin{vmatrix} 0 & 1 & 0 & 3 & 0 & 5 \\ & 0 & 4 & 0 & 8 & 0 \\ & & 0 & 6 & 0 & 10 \\ & & & 0 & 8 & 0 \\ & & & & 0 & 10 \\ & & & & & 0 \end{vmatrix}, \quad \widehat{L}_{sp} \equiv \widehat{D}_T^2 = \begin{vmatrix} 0 & 0 & 4 & 0 & 32 & 0 \\ & 0 & 0 & 24 & 0 & 120 \\ & & 0 & 0 & 48 & 0 \\ & & & 0 & 0 & 80 \\ & & & & 0 & 0 \\ & & & & & 0 \end{vmatrix}. \tag{21}$$

The non-zero entries of $\widehat{D}_T^2$ are

$$\left(\widehat{D}_T^2\right)_{nv} = \frac{v(v^2-n^2)}{c_n}; \quad v = 2, \ldots, N, \ n = v-2, v-4, \ldots, Mod[v, 2], \tag{22}$$

with

$$c_0 = 2, \quad c_n = 1 \quad \text{for } 1 \leqslant n \leqslant N. \tag{23}$$

Eq. (16), together with (15), allow us to evaluate

$$U^{(2)} = \left(u_p^{(2)} \equiv u_N^{(2)}(x_p), p = 0, \ldots, N\right)^t,$$

the physical companion of $\widehat{U}^{(2)}$, and also the derivative operators in physical space, namely

$$U^{(2)} = L_{sp}U \equiv D_T^2 U \quad \text{with } D_T = \mathcal{T} \cdot \widehat{D}_T \cdot \mathcal{T}^{-1}. \tag{24}$$

The D_T^2 matrix is full. For $N = 5$, it reads

$$D_T^2 = \begin{vmatrix} 41.6 & -68.4 & 40.8 & -23.6 & 17.6 & -8 \\ 21.3 & -31.5 & 12.7 & -3.69 & 2.21 & -0.953 \\ -1.85 & 7.32 & -10.1 & 5.79 & -1.91 & 0.714 \\ 0.714 & -1.91 & 5.79 & -10.1 & 7.32 & -1.85 \\ -0.953 & 2.21 & -3.69 & 12.7 & -31.5 & 21.3 \\ -8 & 17.6 & -23.6 & 40.8 & -68.4 & 41.6 \end{vmatrix}.$$

The extreme rows of the D_T^2 matrix are linear combination of the internal rows: they have to be replaced by the boundary conditions for the resulting matrix to be invertible.

3.4.2. Structure of the $\widehat{L}_{app}$ matrix

This matrix represents a polynomial second derivative. Therefore

1. it has a kernel spanned by $T_0(x)$ and $T_1(x)$;
2. it preserves the x-symmetry of the polynomial which it acts on;
3. it reduces by 2 units the degree of any polynomial.

As a consequence, the $\widehat{L}_{app}$ and $\widehat{D}_T^2$ matrices have an identical structure. Let us write, for $N = 5$ for example,

$$\widehat{L}_{app} = \begin{vmatrix} 0 & 0 & \widehat{L}_{02} & 0 & \widehat{L}_{04} & 0 \\ & 0 & 0 & \widehat{L}_{13} & 0 & \widehat{L}_{15} \\ & & 0 & 0 & \widehat{L}_{24} & 0 \\ & & & 0 & 0 & \widehat{L}_{35} \\ & & & & 0 & 0 \\ & & & & & 0 \end{vmatrix}, \tag{25}$$

where the $\widehat{L}_{ij}$ entries depend upon the scheme chosen for the $\frac{d^2}{dx^2}$ approximation. They were analytically identified in [12] for FD2. They are analytically expressed, in Appendix B, for the FE1 and FV1 approximations, from the analytical expression of the stiffness and mass matrices $\widehat{\mathbb{L}}_\bullet$, and using (19).

3.5. Integration matrices

The derivation matrices are not invertible: the eigenvalues of $\widehat{D}_T^2$ and D_T^2 are all zero. How may we nevertheless determine the matrices representing the $\mathcal{L}_{app}^{-1}$ operators which can be understood as performing double integrations? We answer this question first with $\widehat{D}_T^2$. This can then be applied to L_{app}.

3.5.1. Chebyshev double integration

The Chebyshev double integration in pseudo-spectral space is well known [11,1]. It proceeds from the relation

$$\widehat{u}_n = \frac{c_{n-2}}{4n(n-1)}\widehat{u}_{n-2}^{(2)} - \frac{e_{N-(n+2)}}{2(n^2-1)}\widehat{u}_n^{(2)} + \frac{e_{N-(n+4)}}{4n(n+1)}\widehat{u}_{n+2}^{(2)}, \quad n = 2,\dots,N, \tag{26}$$

where

$$e_n = 1 \text{ if } n \geqslant 0; \quad e_n = 0 \text{ if } n < 0. \tag{27}$$

Let us therefore introduce the pseudo-spectrum $\widehat{u}_n^{(-2)}$ of the twice-integrated polynomial $u_N(x)$, together with the column vector

$$\widehat{U}^{(-2)} = \left(\widehat{u}_n^{(-2)}, n = 0,\dots,N\right)^t,$$

obtained from $\widehat{U}$ through the following matrix relation,

$$\widehat{U}^{(-2)} = \widehat{D}_T^{(-2)}\widehat{U}. \tag{28}$$

The $\widehat{D}_T^{(-2)}$ entries are straightforwardly deduced from (26), namely from

$$\widehat{u}_n^{(-2)} = \frac{c_{n-2}}{4n(n-1)}\widehat{u}_{n-2} - \frac{e_{N-(n+2)}}{2(n^2-1)}\widehat{u}_n + \frac{e_{N-(n+4)}}{4n(n+1)}\widehat{u}_{n+2}, \quad n = 2,\dots,N.$$

The matrix $\widehat{D}_T^{(-2)}$ introduced by (28) is thus a partial inverse of $\widehat{D}_T^2$. It verifies the partial-identity relations

$$\widehat{D}_T^{(-2)} \cdot \widehat{D}_T^2 = \widehat{I}_0^{(-2)}, \quad \widehat{D}_T^2 \cdot \widehat{D}_T^{(-2)} = \widehat{I}_N^{(-2)}, \tag{29}$$

with, for $N = 5$ for example,

$$\widehat{D}_T^{(-2)} = \begin{vmatrix} 0 & 0 & 0 & 0 & 0 & 0 \\ 0 & 0 & 0 & 0 & 0 & 0 \\ \frac{1}{4} & 0 & -\frac{1}{6} & 0 & 0 & 0 \\ 0 & \frac{1}{24} & 0 & -\frac{1}{16} & 0 & 0 \\ 0 & 0 & \frac{1}{48} & 0 & 0 & 0 \\ 0 & 0 & 0 & \frac{1}{80} & 0 & 0 \end{vmatrix}$$

and

$$\widehat{I}_0^{(-2)} = \begin{vmatrix} 0 & 0 & 0 & 0 & 0 & 0 \\ 0 & 0 & 0 & 0 & 0 & 0 \\ & & 1 & & & \\ & & & 1 & & \\ & & & & 1 & \\ & & & & & 1 \end{vmatrix}, \quad \widehat{I}_N^{(-2)} = \begin{vmatrix} 1 & & & & & \\ & 1 & & & & \\ & & 1 & & & \\ & & & 1 & & \\ 0 & 0 & 0 & 0 & 0 & 0 \\ 0 & 0 & 0 & 0 & 0 & 0 \end{vmatrix}.$$

Using the second relation in (24) supplies the collocation formulation $D_T^{(-2)}$ of $\widehat{D}_T^{(-2)}$,

$$D_T^{(-2)} = \mathcal{T} \cdot \widehat{D}_T^{(-2)} \cdot \mathcal{T}^{-1},$$

with $\mathcal{T}$ and $\mathcal{T}^{-1}$ given by (15).

3.5.2. Local-approximation double integration, $\widehat{L}_{app}^{(-1)}$

The partial inverse $\widehat{L}_{app}^{(-1)}$ has the structure of $\widehat{D}_T^{(-2)}$, namely, for $N = 6$,

$$\widehat{L}_{app}^{(-1)} = \begin{vmatrix} 0 & 0 & 0 & 0 & 0 & 0 & 0 \\ 0 & 0 & 0 & 0 & 0 & 0 & 0 \\ a_2 & 0 & b_2 & 0 & d_2 & 0 & 0 \\ 0 & a_3 & 0 & b_3 & 0 & 0 & 0 \\ 0 & 0 & a_4 & 0 & b_4 & 0 & 0 \\ 0 & 0 & 0 & a_5 & 0 & 0 & 0 \\ 0 & 0 & 0 & 0 & a_6 & 0 & 0 \end{vmatrix}. \tag{30}$$

Its $(3N-9)$ non-zero entries, $(a_n, n = 2,\ldots,N)$, $(b_n, n = 2,\ldots,N-2)$ and $(d_n, n = 2,\ldots,N-4)$ are determined so as to verify (29). They are given by

$$a_n = \frac{1}{\widehat{L}_{n-2\ n}}, \quad n = 2,\ldots,N; \quad b_n = -a_n \frac{\widehat{L}_{n-2\ n+2}}{\widehat{L}_{n\ n+2}}, \quad n = 2,\ldots,N-2,$$
$$d_n = -\frac{a_n \widehat{L}_{n-2\ n+4} + b_n \widehat{L}_{n\ n+4}}{\widehat{L}_{n+2\ n+4}}, \quad n = 2,\ldots,N-4.$$

3.6. $L_{app}^{-1} L_{sp}$ Chebyshev eigenvalues generic expression

Given both matrices, $\widehat{L}_{app}^{(-1)}$ (see (30)) and $\widehat{L}_{sp} \equiv \widehat{D}_T^2$ (see (22), and (21) for $N = 5$), it is easy to construct $\widehat{L}_{app}^{(-1)} \cdot \widehat{L}_{sp}$. This matrix would coincide with $\widehat{I}_0^{(-2)}$ (see (29)) if the local approximations were replaced by the Chebyshev one. Actually, $\widehat{L}_{app}^{(-1)} \cdot \widehat{L}_{sp}$ appears as an upper triangular matrix whose eigenvalues are therefore its diagonal entries. They read

$$\xi_0 = \xi_1 = 1; \quad \xi_n\left[\widehat{L}_{app}^{(-1)} \widehat{L}_{sp}\right] = \frac{4n(n-1)}{c_{n-2} \widehat{L}_{n-2\ n}}, \quad n = 2,\ldots,N, \tag{31}$$

where the $\widehat{L}_{n-2\ n}$'s are the entries of $\widehat{L}_{app}$ first non-zero codiagonal (see (25)). Both the ξ_0 and ξ_1 eigenvalues are set to *1*, instead of zero which would directly come from $L_{app}^{-1} L_{sp}$. They simply mean that $\mathcal{L}_{app}$ and $\mathcal{L}_{sp}$ have the same kernel, in the same way as for the $L_{app}^{-1} L_{sp}$ Fourier eigenvalues, where the constant eigenmode corresponds to $\xi_0 = 1$.

3.7. 3-Node local approximations

We write down the FD2, FE1 and FV1 *3*-node approximations to $\mathcal{L}[u(x)] = \xi u(x)$, defined at the internal nodes of coordinates x_p, $p = 1,\ldots,N-1$. The reader is invited to consult the Appendix A, Section A.1, for the details regarding the FV1 scheme. A common writing is adopted, viz.

$$(L_S U)_p = \xi^{(\bullet)} \left(L_M^{(\bullet)} U\right)_p, \quad p = 1,\ldots,N-1; \quad \bullet = FD2, FE1, FV1,$$

with

$$(L_S U)_p = \frac{u_{p-1}}{h_p} - \left(\frac{1}{h_p} + \frac{1}{h_{p+1}}\right) u_p + \frac{u_{p+1}}{h_{p+1}}. \tag{32}$$

The mass matrices are successively given by

$$\left(L_M^{(FD2)}U\right)_p = \frac{h_p + h_{p+1}}{2}u_p, \tag{33}$$

$$\left(L_M^{(FE1)}U\right)_p = \frac{1}{6}\left[h_p u_{p-1} + 2(h_p + h_{p+1})u_p + h_{p+1}u_{p+1}\right], \tag{34}$$

and

$$\left(L_M^{(FV1)}U\right)_p = \frac{(x_p - \chi_p)^2}{2h_p}u_{p-1} + \left(\frac{(x_p - \chi_p)(x_p + \chi_p - 2x_{p-1})}{2h_p} + \frac{(x_p - \chi_{p+1})(x_p + \chi_{p+1} - 2x_{p+1})}{2h_{p+1}}\right)u_p + \frac{(x_p - \chi_{p+1})^2}{2h_{p+1}}u_{p+1}. \tag{35}$$

3.8. Chebyshev $L_{app}^{-1}L_{sp}$ eigenvalues, without boundary conditions

Apart from both eigenvalues $\xi_0 = \xi_1 = 1$, obtaining the remaining ones relies on the analytical determination of the $\widehat{\mathbb{L}}_S$ and $\widehat{\mathbb{L}}_M$ matrices presented in details in Appendix B. The resulting FD2, FE1 and FV1 Chebyshev eigenvalues $\xi_n[L_{app}^{-1}L_{sp}]$ are now listed for $n = 2,\ldots,N$, as functions of $a = \frac{\pi}{2N}$,

$$\xi_n^{(FD2)}(a) = \frac{n(n-1)\sin(a)\sin(2a)}{2\sin[(n-1)a]\sin(na)}, \quad n = 2,\ldots,N, \tag{36}$$

$$\xi_n^{(FE1)}(a) = \xi_n^{(FD2)}(a)\left\{\frac{c_{n-2}\cos(a) + \frac{2}{c_{n-2}}\cos[(n-1)a]\cos[(n-2)a]}{3\cos(a)}\right\}, \quad n = 2,\ldots,N, \tag{37}$$

and

$$\xi_n^{(FV1)}(a) = \xi_n^{(FD2)}(a)\left\{\frac{\delta_{n2}}{\cos(a)} + \delta_{n3} + e_{n-4}\frac{2\sin\left(\frac{3a}{2}\right) - \sin\left[(2n-\frac{9}{2})a\right] + \sin\left[(2n-\frac{7}{2})a\right]}{2\cos\left(\frac{a}{2}\right)\sin(2a)}\right\}, \quad n = 2,\ldots,N, \tag{38}$$

δ_{np} being the Kronecker symbol, the c_n and e_n coefficients being, respectively, defined by (23) and (27). The $\xi_n^{(FD2)}(a)$ expression is published in [12]. The first four eigenvectors, $V_n(x)$, of eigenvalues ξ_n, $n = 0,1,2,3$, are simply

$$V_n = T_n(x), \quad n = 0,1,2,3,$$

with

$$\xi_2^{(FD2)}(a) = \xi_2^{(FE1)}(a) = 1, \quad \xi_2^{(FV1)}(a) = \frac{1}{\cos(a)},$$

and

$$\xi_3^{(FD2)}(a) = \xi_3^{(FV1)}(a) = \frac{3\sin(a)}{\sin(3a)}, \quad \xi_3^{(FE1)}(a) = 1.$$

The eigenvalues given by (36)–(38) depend on two parameters, a (or N), and $\frac{n}{N}$ which comes from na and replaces the variable $\eta = nh \in [0,1]$ of the periodic case. It is easy to check that the limit for $a \to 0$ and $na \to \eta\frac{\pi}{2} = nh\frac{\pi}{2}$ of the $\xi_n(a)$'s is given by the eigenvalues (5)–(7) of the periodic case. Defining the maximum $M(N) = \max_{(n=0,\ldots,N)}\xi_n(a)$ and minimum $m(N) = \min_{(n=0,\ldots,N)}\xi_n(a)$, the $L_{app}^{-1}L_{sp}$ spectral radius is

$$r(N) = \frac{M(N) - m(N)}{M(N) + m(N)}.$$

The smaller the value of r, the closer $\mathcal{L}_{app}$ is to $\mathcal{L}_{sp}$. Table 1 shows the convergence of $r(N)$ with N towards the FD2, FE1 and FV1 values of r given in (8) by the Fourier analysis.

Table 1
$r(N)$ for FD2, FE1 and FV1.

N	FD2	FE1	FV1
20	0.4	0.15	0.096
50	0.41	0.167	0.12
100	0.419	0.174	0.137
200	0.421	0.178	0.143
1000	0.4228	0.1807	0.1485
10,000	0.4232	0.1814	0.1497
∞	0.423199	0.181451	0.149813

3.9. $L_{app}^{-1}L_{sp}$ Chebyshev eigenvalues, with Dirichlet boundary conditions

Let us write the following eigenvector relation, in pseudo-spectral space,

$$\widehat{L}_{app}^{(-1)}\widehat{D}_T^2\widehat{U} = \xi\left[\widehat{L}_{app}^{(-1)}\widehat{D}_T^2\right]\widehat{U}.$$

Left multiplying this relation by $\widehat{L}_{app}$ leads to

$$\widehat{I}_N^{(-2)}\widehat{D}_T^2\widehat{U} = \widehat{D}_T^2\widehat{U} = \xi\left[\widehat{L}_{app}^{(-1)}\widehat{D}_T^2\right]\widehat{L}_{app}\widehat{U},$$

with $\widehat{I}_N^{(-2)}$ introduced by (29). There are two eigenvalues, ξ_0 and ξ_1, corresponding to the eigenmodes spanning the $\frac{d^2}{dx^2}$ kernel, a kernel common to $\widehat{L}_{app}$ and $\widehat{D}_T^2$. Let us now consider one of the other eigenvectors $\widehat{U}$, those which span the subspace orthogonal to the kernel. It is easy to construct from $\widehat{U}$ a vector $\widehat{U'}$ verifying the Dirichlet boundary conditions at $x = \pm 1$: it suffices to extend $\widehat{U}$ into the aforementioned kernel, $\widehat{U'} = \widehat{U} + \alpha\widehat{I} + \beta\widehat{X}$ with $\widehat{I} = (\delta_{0p}, p = 0,\ldots,N)^t$, $\widehat{X} = (\delta_{1p}, p = 0,\ldots,N)^t$, α and β being constants to be adjusted for each $\widehat{U}$. In particular, $\alpha = 0$ for the $\widehat{U}$'s which are odd with respect to x, and $\beta = 0$ for the even $\widehat{U}$'s. It is obvious that $\widehat{U'}$ is still an eigenvector of $\widehat{D}_T^2\widehat{U'} = \xi\left[\widehat{L}_{app}^{(-1)}\widehat{D}_T^2\right]\widehat{L}_{app}\widehat{U'}$, corresponding to the same eigenvalues ξ.

4. Conclusion

The 3-node, FD2, FE1, FV1 and FV2, preconditioners of $\frac{d^2}{dx^2}$ are Fourier analyzed. Among them, the FV1 approximation turns out to be the best 3-node preconditioner of the $\frac{d^2}{dx^2}$ spectral solver. This is confirmed by the Chebyshev analysis. The Chebyshev $L_{app}^{-1}L_{sp}$ eigenvalues are real. They (slowly) converge towards the Fourier ones when the polynomial cut-off frequency, N, gets very large. They are also those of the preconditioning $L_{app}^{-1}L_{sp}$ operator when $\mathcal{L}_{app}$ and $\mathcal{L}_{sp}$ are endowed with Dirichlet boundary conditions.

Appendix A. The Finite Volume schemes

This appendix merely brings an extremely brief reminder of the FV (see [9] for instance) approximations to the problem (1). The FV1 scheme is written for a Chebyshev Gauss–Lobatto grid defined on the interval $\mathcal{I}$, (2), by $(N+1)$ nodes located at $x_p = -\cos(p\frac{\pi}{N}), p = 0,\ldots,N$. The second grid is made of the Chebyshev Gauss nodes (Fig. 2) whose coordinates are $\chi_p = -\cos\left(\frac{(2p-1)\pi}{2N}\right), p = 1,\ldots,N$. The mesh sizes are denoted by $h_p = x_p - x_{p-1}$, $p = 1,\ldots,N$. The FV2 scheme is written on a regular grid, of $2N$ nodes located at $x_p = \frac{p}{N}, p = -N,\ldots,N-1$, with $\chi_p = x_p - \frac{h}{2}$, $|p| = 0,\ldots,N-1$, the constant mesh size being $h = \frac{1}{N}$. The FV formulation of (1) is given by

$$\int_{\chi_p}^{\chi_{p+1}}\left(\frac{d^2u}{dx^2} - \xi u\right)dx = 0, \quad p = 1,\ldots,N-1,$$

which supplies the following system

$$\left.\frac{du}{dx}\right|_{\chi_p}^{\chi_{p+1}} - \xi\int_{\chi_p}^{\chi_{p+1}} u\,dx = 0, \quad p = 1,\ldots,N-1. \tag{39}$$

These $(N-1)$ equations provide an exact discretisation of the problem (1). The approximation arises when each term of (39) is evaluated by choosing a numerical approximation $u_N(x)$, namely a piecewise-linear (FV1) or -quadratic (FV2) approximation of $u(x)$ respectively given by the relations (40) and (42).

A.1. Piecewise-Linear Scheme, FV1

The approximation $u_N(x)$ is piecewise linear in each of the N intervals $x \in [x_{p-1}, x_p]$,

$$u_N(x) = \frac{u_p - u_{p-1}}{h_p}x + \frac{x_p u_{p-1} - x_{p-1}u_p}{h_p}, \quad u_p \equiv u_N(x_p),\ p = 1,\ldots,N. \tag{40}$$

The first term of (39) is thus evaluated by using

$$\left.\frac{du_N}{dx}\right|_{\chi_p} = \frac{u_p - u_{p-1}}{h_p}, \quad p = 1,\ldots,N.$$

The second term of (39) involves the $u_N(\chi_p)$'s which are eliminated in terms of the u_p's. To this end, one writes the equality of the slopes on both sides of χ_p,

$$\frac{u_{p-1} - u_N(\chi_p)}{x_{p-1} - \chi_p} = \frac{u_p - u_N(\chi_p)}{x_p - \chi_p}, \quad p = 1,\ldots,N,$$

which supplies

$$u_N(\chi_p) = \frac{(x_p - \chi_p)u_{p-1} - (x_{p-1} - \chi_p)u_p}{h_p}, \quad p = 1, \ldots, N.$$

With a regular grid this relation simplifies, with

$$u_N(\chi_p) = \frac{u_{p-1} + u_p}{2}, \quad |p| = 0, \ldots, N-1. \tag{41}$$

The FV1 approximation of (39) thus becomes

$$\frac{u_{p-1}}{h_p} - \left(\frac{1}{h_p} + \frac{1}{h_{p+1}}\right)u_p + \frac{u_{p+1}}{h_{p+1}} = \xi\left\{\frac{(x_p - \chi_p)^2}{2h_p}u_{p-1} + \frac{(x_p - \chi_{p+1})^2}{2h_{p+1}}u_{p+1} + \left(\frac{(x_p - \chi_p)(x_p + \chi_p - 2x_{p-1})}{2h_p} + \frac{(x_p - \chi_{p+1})(x_p + \chi_{p+1} - 2x_{p+1})}{2h_{p+1}}\right)u_p\right\}.$$

A.2. Piecewise-Quadratic Scheme, FV2

Since this scheme is considered only for its Fourier spectrum, we write it with a uniform grid. The approximation $u_N(x)$ reads

$$u_N(x) = a_p x^2 + b_p x + c_p \tag{42}$$

over each of the $(2N-1)$ intervals $x \in [x_{p-1}, x_{p+1}]$, $|p| = 0, \ldots, N-1$. The coefficients a_p, b_p and c_p are determined in such a way that $u_N(x_q) = u_q$, with $q = p-1, p, p+1$. They are given by

$$\begin{vmatrix} a_p \\ b_p \\ c_p \end{vmatrix} = \frac{1}{2h^2}\begin{vmatrix} 1 & -2 & 1 \\ -(2p+1)h & 4ph & -(2p-1)h \\ p(p+1)h^2 & -2(p^2-1)h^2 & p(p-1)h^2 \end{vmatrix}\begin{vmatrix} u_{p-1} \\ u_p \\ u_{p+1} \end{vmatrix}.$$

The first term of (39) is thus evaluated by using

$$\frac{du_N}{dx}|_{\chi_p} = 2a_p\chi_p + b_p, \quad p = 1, \ldots, N,$$

and the second by

$$\int_{\chi_p}^{\chi_{p+1}} u_N dx = \left(a_p\frac{x^3}{3} + b_p\frac{x^2}{2} + c_p x\right)\Big|_{\chi_p}^{\chi_{p+1}},$$

knowing that $\chi_p = x_p - \frac{h}{2}$. The elimination of the $u_N(\chi_p)$'s in terms of the u_p's is made through the following relation

$$u_N(\chi) = \widehat{A}_p(\chi)u_{p-1} + \widehat{B}_p(\chi)u_p + \widehat{C}_p(\chi)u_{p+1}, \quad \chi = \chi_p, \chi_{p+1}, \ |p| = 0, \ldots, N-1, \tag{43}$$

where

$$\widehat{A}_p(\chi) = \frac{\chi^2 - (2x_p + h)\chi + x_p(x_p + h)}{2h^2}, \quad \widehat{C}_p(\chi) = \frac{\chi^2 - (2x_p - h)\chi + x_p(x_p - h)}{2h^2},$$

together with

$$\widehat{B}_p(\chi) = -\frac{\chi^2 - 2x_p\chi + \left(x_p^2 - h^2\right)}{h^2}.$$

All that leads to (3) and (4).

A.3. How to impose the Dirichlet boundary conditions into the weak formulations of (1)?

It is worth making a comment regarding the way the boundary conditions $u_N(x = \pm 1) = 0$ should be implemented. If the goal is simply to solve the inhomogeneous problem $\frac{d^2u}{dx^2} = f(x)$, then imposing the boundary conditions into the stiffness matrix leads to the right approximation $u_N(x)$. But evaluating correctly the eigenvalues ξ_{app} of these approximations of (1) is quite different. Should one impose the boundary conditions in both stiffness and mass matrices? or in the L_{app} matrix that comes from them by applying (19) and (20)? Proceeding with the former option leads to complex ξ_{app}'s. Only the latter choice preserves the ellipticity of problem (1). The reason is simple: in contrast with the stiffness matrix, the mass matrices are not singular. There is no room for them to take the boundary conditions into account. This requires that the stiffness and mass matrices be known as square $(N+1) \times (N+1)$ matrices: determining them through their pseudo-spectral formulation thus reveals itself as being extremely useful.

Appendix B. Analytical determination of $\widehat{\mathbb{L}}_S$, $\widehat{\mathbb{L}}_M^{(\bullet)}$ and $\hat{L}^{(\bullet)}$, and of the $\xi_{\boldsymbol{n}}^{(\bullet)}(\boldsymbol{a})$, for $\bullet$ = FD2, FE1, FV1

B.1. Some formulae

These are useful relations for the forthcoming trigonometrical transformations. From

$$x_p = -\cos(\theta_p), \quad \theta_p = p\frac{\pi}{N}, \quad p = 0,\ldots,N,$$

one has

$$h_p = x_p - x_{p-1} = 2\sin(a)\sin(\theta_p - a), \quad p = 1,\ldots,N,$$

and

$$h_p + h_{p+1} = 2\sin(2a)\sin(\theta_p), \quad p = 1,\ldots,N-1, \tag{44}$$

where

$$a = \frac{\pi}{2N}.$$

We will have to express matrix entries of the kind $(L_\bullet \mathcal{T})_{pn}$ (see (18)). To this end, let us write

$$T_n(x_{p\pm1}) - T_n(x_p) = \mp 2(-1)^n \sin(na)\sin\left[n(\theta_p \pm a)\right], \quad p = 1,\ldots,N-1,$$

and

$$T_n(x_{p\pm1}) + T_n(x_p) = 2(-1)^n \cos(na)\cos\left[n(\theta_p \pm a)\right], \quad p = 1,\ldots,N-1.$$

According to (12) the Gauss node coordinates are

$$\chi_p = -\cos\left(\frac{(2p-1)\pi}{2N}\right) = -\cos(\theta_p - a), \quad \chi_{p+1} = -\cos(\theta_p + a), \quad p = 1,\ldots,N.$$

Let us introduce the Chebyshev polynomials of the second kind, [20]. Given the definition $x = -\cos(\theta)$, they read

$$U_n(x) = \frac{1}{n+1}\frac{dT_{n+1}}{dx} = (-1)^n \frac{\sin\left((n+1)\theta\right)}{\sin(\theta)}, \quad n \geqslant 0. \tag{45}$$

Their Chebyshev spectrum is given by

$$U_n(x) = 2\sum_{\substack{j=Mod[n,2]\\ \Delta j=2}}^{n} \frac{T_j(x)}{c_j}, \quad n \geqslant 0, \tag{46}$$

with the c_j's defined by (23).

B.2. $\widehat{\mathbb{L}}_S$ analytical determination

Let us start from the relation (32) which gives, for $n = 0,\ldots,N$,

$$(L_S\mathcal{T})_{pn} = \frac{T_n(x_{p-1}) - T_n(x_p)}{h_p} + \frac{T_n(x_{p+1}) - T_n(x_p)}{h_{p+1}}, \quad p = 1,\ldots,N-1.$$

This can be written as

$$(L_S\mathcal{T})_{pn} = (-1)^n \frac{\sin(na)}{\sin(a)}\left\{\frac{\sin\left[n(\theta_p - a)\right]}{\sin\left(\theta_p - a\right)} - \frac{\sin\left[n(\theta_p + a)\right]}{\sin\left(\theta_p + a\right)}\right\}, \quad p = 1,\ldots,N-1. \tag{47}$$

Noting that the term between brackets in (47) is proportional to $[U_{n-1}(x_+) - U_{n-1}(x_-)]$, with $x_\pm = -\cos(\theta_p \pm a)$, leads to

$$(L_S\mathcal{T})_{pn} = \frac{\sin(na)}{\sin(a)}[U_{n-1}(x_+) - U_{n-1}(x_-)]. \tag{48}$$

By (46) one has, for $n \geqslant 1$,

$$U_{n-1}(x_+) - U_{n-1}(x_-) = 2\sum_{\substack{j=Mod[n-1,2],\\ \Delta j=2}}^{n-1} \frac{T_j(x_+) - T_j(x_-)}{c_j} = -4\sum_{\substack{j=Mod[n-1,2],\\ \Delta j=2}}^{n-1} (-1)^j \sin(ja)\sin(j\theta_p).$$

The expression (48) then becomes, still for $n = 0,\ldots,N$,

$$(L_S\mathcal{T})_{pn} = -\frac{4\sin(na)}{\sin(a)}\sum_{\substack{j=Mod[n-1,2],\\ \Delta j=2}}^{n-1} (-1)^j \sin(ja)\sin(j\theta_p), \quad p = 1,\ldots,N-1.$$

The $U_{j-1}(x)$'s can again be introduced in this r.h.s. and replaced by their expansion (46). After some more manipulations one is left with the following expression,

$$(L_S\mathcal{T})_{pn} = \frac{8\sin(na)}{\sin(a)}\sin(\theta_p)\sum_{\substack{q=Mod[n,2],\\ \Delta q=2}}^{n-2}\left[\sum_{\substack{j=q+1,\\ \Delta j=2}}^{n-1}\sin(ja)\right]\frac{T_q(x_p)}{c_q},\quad p=1,\ldots,N-1.$$

Identifying this relation with (18) supplies the $\widehat{\mathbb{L}}_S$ non-zero entries. They read

$$\left(\widehat{\mathbb{L}}_S\right)_{qn} = \frac{8\sin(na)}{c_q\sin(a)}\sum_{\substack{j=q+1,\\ \Delta j=2}}^{n-1}\sin(ja);\quad n=2,\ldots,N;\ q=Mod[n,2],\ldots,n-2,\ \Delta q=2. \tag{49}$$

B.3. $\widehat{\mathbb{L}}_M^{(FD2)}$ and $\widehat{L}^{(FD2)}$ analytical determination

Starting from (33), and using (44) together with (18), straightforwardly lead to $\widehat{\mathbb{L}}_M^{(FD2)}$. This matrix is diagonal, with

$$\left(\widehat{\mathbb{L}}_M^{(FD2)}\right)_{qn} = \sin(2a)\delta_{qn}. \tag{50}$$

Thus, by (19), we can write down the $\widehat{L}^{(FD2)}$ matrix non-zero entries,

$$\widehat{L}^{(FD2)}_{qn} = \frac{8}{c_q}\frac{\sin(na)}{\sin(a)\sin(2a)}\sum_{\substack{j=q+1,\\ \Delta j=2}}^{n-1}\sin(ja);\quad n=2,\ldots,N;\ q=Mod[n,2],\ldots,n-2,\ \Delta q=2.$$

For $N=5$, the matrix $\widehat{L}^{(FD2)}$ and its collocation version $L^{(FD2)}$ read

$$\widehat{L}^{(FD2)} = \begin{vmatrix} 0 & 0 & 4 & 0 & 23.4 & 0 \\ & 0 & 0 & 20.9 & 0 & 67.8 \\ & & 0 & 0 & 33.9 & 0 \\ & & & 0 & 0 & 41.9 \\ & & & & 0 & 0 \\ & & & & & 0 \end{vmatrix},$$

and

$$L^{(FD2)} = \begin{vmatrix} 27.4 & -42.6 & 20.9 & -9.37 & 6.47 & -2.89 \\ 15.2 & -20.9 & 5.79 & & & \\ & 3.58 & -6.47 & 2.89 & & \\ & & 2.89 & -6.47 & 3.58 & \\ & & & 5.79 & -20.9 & 15.2 \\ -2.89 & 6.47 & -9.37 & 20.9 & -42.6 & 27.4 \end{vmatrix}. \tag{51}$$

One sees that $\widehat{L}^{(FD2)}$ does have the structure announced in Section 3.4.2. As regards the collocation matrix, $L^{(FD2)}$, one recognizes the expected tridiagonal part. Its extreme rows are linear combinations of the others, obtained by evaluating $(L^{(FD2)}\mathcal{T})_{pn}$ at the boundary nodes, $p=0,N$. It is easy to check that

$$\left(L^{(FD2)}\mathcal{T}\right)_{0n} = (-1)^n\left(L^{(FD2)}\mathcal{T}\right)_{Nn} = \frac{2\sin(na)}{\sin^3(a)\sin(2a)}[\cos(a)\sin(na) - n\sin(a)\cos(na)],\quad n=0,\ldots,N.$$

Replacing the last two rows of zeros of $\widehat{L}^{(FD2)}$ by the TAU boundary conditions, or the extreme rows of $L^{(FD2)}$ by the physical boundary conditions, leads respectively to the pseudo-spectral or collocation formulation of the $\frac{d^2}{dx^2}$ FD2 solver.

B.4. $\widehat{\mathbb{L}}_M^{(FE1)}$ and $\widehat{L}^{(FE1)}$ analytical determination

B.4.1. $\widehat{\mathbb{L}}_M^{(FE1)}$ analytical determination

Let us write the entries $\left(\widehat{L}_M^{(FE1)}\mathcal{T}\right)_{pn}$, following (34), for $n=0,\ldots,N$, as follows,

$$\left(\widehat{L}_M^{(FE1)}\mathcal{T}\right)_{pn} = \frac{1}{6}\{h_p[T_n(x_{p-1}) + T_n(x_p)] + (h_p + h_{p+1})T_n(x_p) + h_{p+1}[T_n(x_{p+1}) + T_n(x_p)]\},\quad p=1,\ldots,N-1. \tag{52}$$

For $n \geqslant 2$ some trigonometric manipulations lead to

$$\left(\widehat{L}_M^{(FE1)}\mathcal{T}\right)_{pn} = \frac{2\sin(a)}{3}\sin(\theta_p)\{\cos(a)T_n(x_p) + \cos(na)[\cos((n+1)a)U_n(x_p) - \cos((n-1)a)U_{n-2}(x_p)]\}, \quad p = 1,\ldots,N-1,$$

noting that, for $n = 0,1$, one has from (52)

$$\left(\widehat{L}_M^{(FE1)}\right)_{p0} = \sin(2a)T_0(x_p)\sin(\theta_p), \quad p = 1,\ldots,N-1,$$

and

$$\left(\widehat{L}_M^{(FE1)}\right)_{p1} = \frac{\sin(2a)}{3}[1 + 2\cos(2a)]T_1(x_p)\sin(\theta_p), \quad p = 1,\ldots,N-1.$$

Identifying these three expressions with (18) supplies the following non-zero entries of $\widehat{\mathbb{L}}_M^{(FE1)}$,

$$\left(\widehat{\mathbb{L}}_M^{(FE1)}\right)_{qn} = \frac{2\sin(a)}{3}\left\{\delta_{qn}c_n\cos(a) + \frac{2}{c_q}\cos(na)[\cos((n+1)a) - e_{n-2-q}\cos((n-1)a)]\right\}, \quad n = 0,\ldots,N;\ q = Mod[n,2],\ldots,n,\ \Delta q = 2. \tag{53}$$

It is easy to check that the last-column entries, $(\widehat{\mathbb{L}}_M^{(FE1)})_{qN}$, except the diagonal one, cancel. For $N = 5$, this matrix reads

$$\widehat{\mathbb{L}}_M^{(FE1)} = \frac{1}{10}\begin{vmatrix} 5.88 & 0 & -0.61 & 0 & -0.37 & 0 \\ 0 & 5.13 & 0 & -1.21 & 0 & 0 \\ 0 & 0 & 3.92 & 0 & -0.75 & 0 \\ 0 & 0 & 0 & 2.71 & 0 & 0 \\ 0 & 0 & 0 & 0 & 1.96 & 0 \\ 0 & 0 & 0 & 0 & 0 & 1.96 \end{vmatrix}. \tag{54}$$

It is invertible.

B.4.2. $\widehat{L}^{(FE1)}$ matrix

Applying now the relation (19) with (49) and (54) provides this matrix. Its collocation partner, $L^{(FE1)}$, can then be computed. They are, for $N = 5$,

$$\widehat{L}^{(FE1)} = \begin{vmatrix} 0 & 0 & 4 & 0 & 28.7 & 0 \\ & 0 & 0 & 24 & 0 & 99.1 \\ & & 0 & 0 & 50.8 & 0 \\ & & & 0 & 0 & 90.9 \\ & & & & 0 & 0 \\ & & & & & 0 \end{vmatrix},$$

and

$$L^{(FE1)} = \begin{vmatrix} 40.5 & -66.2 & 38.8 & -21.7 & 15.8 & -7.11 \\ 18.8 & -26.7 & 8.33 & 0.0522 & -1.04 & 0.579 \\ -4.5 & 12.2 & -13.8 & 8.15 & -3.14 & 1.12 \\ 1.12 & -3.14 & 8.15 & -13.8 & 12.2 & -4.5 \\ 0.579 & -1.04 & 0.0522 & 8.33 & -26.7 & 18.8 \\ -7.11 & 15.8 & -21.7 & 38.8 & -66.2 & 40.5 \end{vmatrix}. \tag{55}$$

This $\frac{d^2}{dx^2}$ approximation matrix is full, its two extreme rows being linear combination of the interior ones.

B.5. $\widehat{\mathbb{L}}_M^{(FV1)}$ and $\widehat{L}^{(FV1)}$ analytical determination

B.5.1. $\widehat{\mathbb{L}}_M^{(FV1)}$ analytical determination

As regards $(\widehat{L}_M^{(FV1)}\mathcal{T})_{pn}$, let us reorganize and split the writing of $(L_M^{(FV1)}U)_p$ as given by (35) as follows:

$$\left(\widehat{L}_M^{(FV1)}\mathcal{T}\right)_{pn} = \sum_{i=1}^{3}\left\{\left(\widehat{L}_M^{(FV1)}\mathcal{T}\right)_{pn}\right\}_i \quad \text{for}\begin{cases} p = 1,\ldots,N-1, \\ n = 0,\ldots,N, \end{cases} \tag{56}$$

where

$$\left\{\left(\widehat{L}_M^{(FV1)}\mathcal{T}\right)_{pn}\right\}_1 = \left(T_n(x_p) - T_n(x_{p-1})\right)\left(\frac{x_p^2 - \chi_p^2}{2h_p}\right) + \left(T_n(x_{p+1}) - T_n(x_p)\right)\left(\frac{\chi_{p+1}^2 - x_p^2}{2h_{p+1}}\right),$$
$$\left\{\left(\widehat{L}_M^{(FV1)}\mathcal{T}\right)_{pn}\right\}_2 = \left(x_p T_n(x_{p-1}) - x_{p-1}T_n(x_p)\right)\left(\frac{x_p - \chi_p}{h_p}\right),$$

and

$$\left\{\left(\widehat{L}_M^{(FV1)}\mathcal{T}\right)_{pn}\right\}_3 = \left(x_{p+1}T_n(x_p) - x_p T_n(x_{p+1})\right)\left(\frac{\chi_{p+1} - x_p}{h_{p+1}}\right).$$

This system involves the following new quantities, for $p = 1,\ldots,N-1$,

$$\frac{x_p - \chi_p}{h_p} = \frac{\sin\left(\theta_p - \frac{a}{2}\right)}{2\cos\left(\frac{a}{2}\right)\sin\left(\theta_p - a\right)}, \quad \frac{\chi_{p+1} - x_p}{h_{p+1}} = \frac{\sin\left(\theta_p + \frac{a}{2}\right)}{2\cos\left(\frac{a}{2}\right)\sin\left(\theta_p + a\right)},$$
$$\frac{x_p^2 - \chi_p^2}{2h_p} = -\frac{\sin\left(2\theta_p - a\right)}{4\sin(\theta_p - a)}, \quad \frac{\chi_{p+1}^2 - x_p^2}{2h_{p+1}} = -\frac{\sin(2\theta_p + a)}{4\sin(\theta_p + a)},$$

$$x_p T_n(x_{p-1}) - x_{p-1}T_n(x_p) = (-1)^{n+1}\left\{\sin\left[(n+1)(\theta_p - a)\right]\sin\left[(n-1)a\right] + \sin\left[(n-1)(\theta_p - a)\right]\sin\left[(n+1)a\right]\right\},$$

and

$$x_{p+1}T_n(x_p) - x_p T_n(x_{p+1}) = (-1)^{n+1}\left\{\sin\left[(n+1)(\theta_p + a)\right]\sin\left[(n-1)a\right] + \sin\left[(n-1)(\theta_p + a)\right]\sin\left[(n+1)a\right]\right\}.$$

Taking them into account successively yields, for $n = 0,\ldots,N$,

$$\left\{\left(\widehat{L}_M^{(FV1)}\mathcal{T}\right)_{pn}\right\}_1 = (-1)^n\frac{\sin(na)}{2}\left[\sin(2\theta_p - a)\frac{\sin[n(\theta_p - a)]}{\sin(\theta_p - a)} + \sin(2\theta_p + a)\frac{\sin[n(\theta_p + a)]}{\sin(\theta_p + a)}\right],$$
$$p = 1,\ldots,N-1,$$
$$\left\{\left(\widehat{L}_M^{(FV1)}\mathcal{T}\right)_{pn}\right\}_2 = (-1)^{n+1}\frac{\sin[(n-1)a]}{2\cos\left(\frac{a}{2}\right)}\left[\sin\left(\theta_p - \frac{a}{2}\right)\frac{\sin[(n+1)(\theta_p - a)]}{\sin(\theta_p - a)} + \sin\left(\theta_p + \frac{a}{2}\right)\frac{\sin[(n+1)(\theta_p + a)]}{\sin(\theta_p + a)}\right],$$
$$p = 1,\ldots,N-1,$$
$$\left\{\left(\widehat{L}_M^{(FV1)}\mathcal{T}\right)_{pn}\right\}_3 = (-1)^{n+1}\frac{\sin[(n+1)a]}{2\cos\left(\frac{a}{2}\right)}\left[\sin\left(\theta_p - \frac{a}{2}\right)\frac{\sin[(n-1)(\theta_p - a)]}{\sin(\theta_p - a)} + \sin\left(\theta_p + \frac{a}{2}\right)\frac{\sin[(n-1)(\theta_p + a)]}{\sin(\theta_p + a)}\right],$$
$$p = 1,\ldots,N-1.$$

A non-zero contribution for $n = 0$ only comes from the last two terms of (56), while only the first term of (56) is involved for $n = 1$. All that reads, still for $p = 1,\ldots,N-1$,

$$\left(\widehat{L}_M^{(FV1)}\mathcal{T}\right)_{p0} = \sum_{i=2}^{3}\left\{\left(\widehat{L}_M^{(FV1)}\mathcal{T}\right)_{p0}\right\}_i = 2\sin(a)\sin(\theta_p)T_0(x_p), \quad \left(\widehat{L}_M^{(FV1)}\mathcal{T}\right)_{p1} = \left\{\left(\widehat{L}_M^{(FV1)}\mathcal{T}\right)_{p1}\right\}_1$$
$$= \sin(2a)\sin(\theta_p)T_1(x_p). \tag{57}$$

The forthcoming final expression of $(\widehat{L}_M^{(FV1)}\mathcal{T})_{pn}$ will have to agree with both these particular cases.

The $U_n(x)$'s (see (45)) which appear in the $\{(\widehat{L}_M^{(FV1)}\mathcal{T})_{pn}\}_i$'s are now transformed through (46), which leads to the following relations,

$$\left\{\left(\widehat{L}_M^{(FV1)}\mathcal{T}\right)_{pn}\right\}_1 = \sum_{\substack{j=Mod[n-1,2],\\ \Delta j=2}}^{n-1}(-1)^j\left[(A_1)_{nj}\sin[(j+2)\theta_p] + (B_1)_{nj}\sin[(j-2)\theta_p]\right], \quad n = 1,\ldots,N;\ p = 1,\ldots,N-1,$$

where

$$(A_1, B_1)_{nj} = -\frac{\sin(na)}{c_j}\{\cos[(j+1)a], -\cos[(j-1)a]\};$$
$$\left\{\left(\widehat{L}_M^{(FV1)}\mathcal{T}\right)_{pn}\right\}_2 = -\sum_{\substack{j=Mod[n,2],\\ \Delta j=2}}^{n}(-1)^j\left[(A_2)_{nj}\sin[(j+1)\theta_p] + (B_2)_{nj}\sin[(j-1)\theta_p]\right], \quad n = 0,\ldots,N;\ p = 1,\ldots,N-1,$$

where

$$(A_2,B_2)_{nj}=\frac{\sin[(n-1)a]}{\cos\left(\frac{a}{2}\right)}\frac{c_n}{c_j}\left(\cos\left[\left(j+\frac{1}{2}\right)a\right],-\cos\left[\left(j-\frac{1}{2}\right)a\right]\right);$$

$$\left\{\left(\widehat{L}_M^{(FV1)}\mathcal{T}\right)_{pn}\right\}_3=-\sum_{\substack{j=Mod[n,2],\\ \Delta j=2}}^{n-2}(-1)^j\Big[(A_3)_{nj}\sin[(j+1)\theta_p]+(B_3)_{nj}\sin[(j-1)\theta_p]\Big],\quad n=2,\ldots,N;\ p=1,\ldots,N-1,$$

where

$$(A_3,B_3)_{nj}=\frac{\sin[(n+1)a]}{\cos\left(\frac{a}{2}\right)}\frac{1}{c_j}\left(\cos\left[\left(j+\frac{1}{2}\right)a\right],-\cos\left[\left(j-\frac{1}{2}\right)a\right]\right).$$

The coefficient c_n is inserted into the expression for $(A_2,B_2)_{nj}$ in order to recover the right value (57) of $(\widehat{L}_M^{(FV1)}\mathcal{T})_{p0}$. Notice that $\{(\widehat{L}_M^{(FV1)}\mathcal{T})_{p1}\}_1$ gives the right value (57) of $(\widehat{L}_M^{(FV1)}\mathcal{T})_{p1}$.

With a view to gathering these sums into a unique sum, an intermediate transformation is made, leading to

$$\left\{\left(\widehat{L}_M^{(FV1)}\mathcal{T}\right)_{pn}\right\}_1=\sum_{\substack{j=1+Mod[n,2],\\ \Delta j=2}}^{n+1}(-1)^j\sin(j\theta_p)\Big[e_{j-2}(A_1)_{n\ j-2}+e_{n-3-j}(B_1)_{n\ j+2}-\delta_{j1+Mod[n,2]}(B_1)_{n\ 2-j}\Big],$$

$$n=1,\ldots,N;\ p=1,\ldots,N-1,$$

$$\left\{\left(\widehat{L}_M^{(FV1)}\mathcal{T}\right)_{pn}\right\}_2=\sum_{\substack{j=1+Mod[n,2],\\ \Delta j=2}}^{n+1}(-1)^j\sin(j\theta_p)\Big[(A_2)_{n\ j-1}+e_{n-1-j}(B_2)_{n\ j+1}-\delta_{n\ 2q}\delta_{j1}(B_2)_{n0}\Big],$$

$$n=0,\ldots,N;\ p=1,\ldots,N-1,$$

$$\left\{\left(\widehat{L}_M^{(FV1)}\mathcal{T}\right)_{pn}\right\}_3=\sum_{\substack{j=1+Mod[n,2],\\ \Delta j=2}}^{n+1}(-1)^j\sin(j\theta_p)\Big[e_{n-1-j}(A_3)_{n\ j-1}+e_{n-3-j}(B_3)_{n\ j+1}-\delta_{n\ 2q}\delta_{j1}(B_3)_{n0}\Big],$$

$$n=2,\ldots,N;\ p=1,\ldots,N-1,$$

where q is any positive integer. Whence the unique sum,

$$\left(\widehat{L}_M^{(FV1)}\mathcal{T}\right)_{pn}=\sum_{\substack{j=1+Mod[n,2],\\ \Delta j=2}}^{n+1}(-1)^j\mathcal{A}_{nj}\sin(j\theta_p),\quad n=0,\ldots,N;\ p=1,\ldots,N-1,\tag{58}$$

with

$$\begin{aligned}\mathcal{A}_{nj}=&\,e_{n-1}\Big[e_{j-2}(A_1)_{n\ j-2}+e_{n-3-j}(B_1)_{n\ j+2}-\delta_{j1+Mod[n,2]}(B_1)_{n2-j}\Big]e_{n-1-j}(B_2)_{n\ j+1}+(A_2)_{n\ j-1}-\delta_{n\ 2q}\delta_{j1}(B_2)_{n0}\\&+e_{n-2}\Big[e_{n-1-j}(A_3)_{n\ j-1}+e_{n-3-j}(B_3)_{n\ j+1}-\delta_{n\ 2q}\delta_{j1}(B_3)_{n0}\Big].\end{aligned}\tag{59}$$

At last, the relation (58) is transformed according to

$$\left(\widehat{L}_M^{(FV1)}\mathcal{T}\right)_{pn}=-\sin(\theta_p)\sum_{\substack{j=Mod[n,2],\\ \Delta j=2}}^{n}\mathcal{A}_{nj+1}U_j(x_p),\quad n=0,\ldots,N;\ p=1,\ldots,N-1,$$

which leads to the matrix $\widehat{\mathbb{L}}_M^{(FV1)}$ whose non-zero entries read

$$\left(\widehat{\mathbb{L}}_M^{(FV1)}\right)_{qn}=-\frac{2}{c_q}\sum_{j=q+1,\Delta j=2}^{n+1}\mathcal{A}_{nj};\quad n=0,\ldots,N,\ q=Mod[n,2],\ldots,n,\ \Delta q=2.\tag{60}$$

For $N=5$ this matrix is

$$\widehat{\mathbb{L}}_M^{(FV1)}=\frac{1}{10}\begin{vmatrix}6.18 & 0 & 0.0282 & 0 & 0.165 & 0\\ & 5.88 & 0 & 0.147 & 0 & 0.477\\ & & 5.09 & 0 & 0.239 & 0\\ & & & 4.11 & 0 & 0.295\\ & & & & 3.32 & 0\\ & & & & & 3.01\end{vmatrix}.\tag{61}$$

B.5.2. $\widehat{L}^{(FV1)}$ *matrix*

Applying (19) with (49) and (61) provides this matrix. Its collocation partner, $L^{(FV1)}$, can also be computed. These matrices are, for $N = 5$,

$$\widehat{L}^{(FV1)} = \begin{vmatrix} 0 & 0 & 3.8 & 0 & 22.1 & 0 \\ & 0 & 0 & 20.9 & 0 & 66.3 \\ & & 0 & 0 & 39.2 & 0 \\ & & & 0 & 0 & 59.9 \\ & & & & 0 & 0 \\ & & & & & 0 \end{vmatrix},$$

and

$$L^{(FV1)} = \begin{vmatrix} 29.8 & -47.2 & 24.8 & -12.1 & 8.48 & -3.8 \\ 14.5 & -19.7 & 4.53 & 1.46 & -1.48 & 0.702 \\ -2.67 & 8.38 & -10.1 & 5.28 & -1.23 & 0.35 \\ 0.35 & -1.23 & 5.28 & -10.1 & 8.38 & -2.67 \\ 0.702 & -1.48 & 1.46 & 4.53 & -19.7 & 14.5 \\ -3.8 & 8.48 & -12.1 & 24.8 & -47.2 & 29.8 \end{vmatrix}. \tag{62}$$

B.6. The $\xi_n^{(\bullet)}(a), \bullet = FD2, FE1, FV1$

All the matrices are known. Their particular structure allows us to write down a simple relation between $\xi_n^{(FE1)}(a)$, $\xi_n^{(FV1)}(a)$ and $\xi_n^{(FD2)}(a)$.

By (31), only the $\widehat{L}^{(\bullet)}_{n-2\ n}$ entries are involved in the $\xi_n^{(\bullet)}(a)$ analytical expression. Then, making use of (19), one gets

$$\widehat{L}^{(\bullet)}_{n-2\ n} = \frac{\left(\widehat{\mathbb{L}}_S\right)_{n-2\ n}}{\left(\widehat{\mathbb{L}}^{(\bullet)}_M\right)_{n-2\ n-2}}, \quad n = 2, \ldots, N,$$

and therefore

$$\xi_n^{(\bullet)}(a) = \frac{4n(n-1)\left(\widehat{\mathbb{L}}^{(\bullet)}_M\right)_{n-2\ n-2}}{c_{n-2}\left(\widehat{\mathbb{L}}_S\right)_{n-2\ n}}, \quad n = 2, \ldots, N. \tag{63}$$

B.6.1. $\xi_n^{(FD2)}(a)$ *analytical expression*

Inserting (50) into (63) gives

$$\xi_n^{(FD2)}(a) = \frac{4n(n-1)\sin(2a)}{c_{n-2}\left(\widehat{\mathbb{L}}_S\right)_{n-2\ n}}, \quad n = 2, \ldots, N. \tag{64}$$

Then, using (49) leads to the eigenvalues given by (36) and published in [12].

B.6.2. $\xi_n^{(FE1)}(a)$ *and* $\xi_n^{(FV1)}(a)$ *general expression*

Comparing (63) with (64) leads to the following simple expression of these eigenvalues,

$$\xi_n^{(\bullet)}(a) = \xi_n^{(FD2)}(a)\frac{\left(\widehat{\mathbb{L}}^{(\bullet)}_M\right)_{n-2\ n-2}}{\sin(2a)}, \quad n = 2, \ldots, N;\ \bullet = FE1, FV1. \tag{65}$$

B.6.3. $\xi_n^{(FE1)}(a)$ *analytical expression*

By (65), the useful $\widehat{\mathbb{L}}_M^{(FE1)}$ entries (see (60)) are

$$\left(\widehat{\mathbb{L}}_M^{(FE1)}\right)_{n-2\ n-2} = \frac{2\sin(a)}{3}\left\{c_{n-2}\cos(a) + \frac{2}{c_{n-2}}\cos[(n-1)a]\cos[(n-2)a]\right\}, \quad n = 2, \ldots, N.$$

This leads to the relation (37) for the $\xi_n^{(FE1)}(a)$ eigenvalues.

B.6.4. $\xi_n^{(FV1)}(a)$ analytical expression

By (65) the useful $\widehat{\mathbb{L}}_M^{(FV1)}$ entries (see (60)) are

$$\left(\widehat{\mathbb{L}}_M^{(FV1)}\right)_{n-2\ n-2} = -\frac{2}{c_{n-2}}\mathcal{A}_{n-2\ n-1}, \quad n = 2,\ldots,N,$$

where, by (59),

$$\mathcal{A}_{n-2\ n-1} = -\delta_{n2}(B_2)_{00} - \delta_{n3}(B_1)_{10} + e_{n-3}(A_1)_{n-2\ n-3} + (A_2)_{n-2\ n-2}.$$

From the definitions given above of the coefficients A_1, A_2, B_1 and B_2, one has

$$\mathcal{A}_{01} = -2\sin(a), \quad \mathcal{A}_{12} = -\frac{\sin(2a)}{2},$$

and

$$\mathcal{A}_{n-2\ n-1} = -\frac{2\sin(\frac{3a}{2}) - \sin\left[(2n-\frac{9}{2})a\right] + \sin\left[(2n-\frac{7}{2})a\right]}{4\cos\left(\frac{a}{2}\right)} \equiv \frac{f_n(a)}{4\cos\left(\frac{a}{2}\right)}, \quad n = 4,\ldots,N,$$

which leads to

$$\left(\widehat{\mathbb{L}}_M^{(FV1)}\right)_{n-2\ n-2} = 2\delta_{n2}\sin(a) + \delta_{n3}\sin(2a) - e_{n-4}\frac{f_n(a)}{2\cos\left(\frac{a}{2}\right)}, \quad n = 2,\ldots,N,$$

and then, through (65), to the relation (38) for the $\xi_n^{(FV1)}(a)$ eigenvalues.

References

[1] C. Canuto, M.Y. Hussaini, A. Quarteroni, T.A. Zang, Spectral Methods in Fluid Dynamics, Springer Series in Computational Physics, Springer-Verlag, New York, 1988.
[2] C. Canuto, A. Quarteroni, Preconditioner minimal residual methods for Chebyshev spectral calculations, J. Comput. Phys. 60 (1985) 315–337.
[3] V. Delgado, G. Kasperski, G. Labrosse, Spectrally accurate numerical incompressible flows with deformed boundaries: a finite volume preconditioning method, J. Comput. Appl. Math. 168 (2004) 145–154.
[4] P. Demaret, M.O. Deville, Chebyshev pseudospectral solution of the Stokes equations using finite element preconditioning, J. Comput. Phys. 83 (1989) 463–484.
[5] P. Demaret, M.O. Deville, Chebyshev collocation solutions of the Navier–Stokes equations using multi-domain decomposition and finite element preconditioning, J. Comput. Phys. 95 (1995) 359–386.
[6] P. Demaret, M.O. Deville, C. Schneidesch, Thermal convection solutions by Chebyshev pseudospectral multi-domain decomposition and finite element preconditioning, Appl. Numer. Math. 6 (1989) 107–121.
[7] M.O. Deville, E.H. Mund, Chebyshev pseudospectral solution of second-order elliptic equations with finite element preconditioning, J. Comput. Phys. 60 (1985) 517–533.
[8] M.O. Deville, E.H. Mund, Fourier analysis of finite element preconditioning collocation schemes, SIAM J. Sci. Stat. Comput. 13 (1992) 596–610.
[9] C.A.J. Fletcher, Computational Techniques for Fluid Dynamics 1, Scientific Computation in Springer Series in Computational Physics, Springer-Verlag, New York, 1996.
[10] P. Francken, M.O. Deville, E.H. Mund, On the spectrum of the iteration operator associated to the finite element preconditioning of Chebyshev collocation calculations, Comp. Methods Appl. Mech. Engrg. 80 (1990) 295–304.
[11] D. Gottlieb, S.A. Orszag, Numerical Analysis of Spectral Methods: Theory and Applications, SIAM-CBMS, Philadelphia, 1977.
[12] P. Haldenwang, G. Labrosse, S. Abboudi, M.O. Deville, Chebyshev 3-d spectral and 2-d pseudospectral solvers for the Helmholtz equation, J. Comput. Phys. 55 (1984) 115–128.
[13] S.D. Kim, S.V. Parter, Preconditioning Chebyshev spectral collocation method for elliptic partial differential equations, SIAM J. Numer. Anal. 33 (6) (1996) 2375–2400.
[14] S.D. Kim, S.V. Parter, Preconditioning Chebyshev spectral collocation by finite-difference operators, SIAM J. Numer. Anal. 34 (3) (1997) 939–958.
[15] E. Leriche, S. Gavrilakis, Direct numerical simulation of the flow in a lid-driven cubical cavity, Phys. Fluids 12 (6) (2000) 1363–1376.
[16] E. Leriche, G. Labrosse, Stokes eigenmodes in square domain and the stream function–vorticity correlation, J. Comput. Phys. 200 (2004) 489–511.
[17] E. Leriche, G. Labrosse, Vector potential–vorticity relationship for the Stokes flows: application to the Stokes eigenmodes in 2D/3D closed domain, Theor. Comp. Fluid Dynamics 21 (1) (2007) 1–13.
[18] A.R. Mitchell, Computational Methods in Partial Differential Equations, John Wiley & Sons, Inc., New York, 1977.
[19] S.A. Orszag, Spectral methods for problems in complex geometries, J. Comput. Phys. 37 (1980) 70–92.
[20] T.J. Rivlin, Chebyshev Polynomials, John Wiley & Sons, Inc., New York, 1990.
[21] F. Thomasset, Implementation of Finite Element Methods for Navier–Stokes Equations, Springer Series in Computational Physics, Springer-Verlag, New York, 1981.
[22] R. Vichnevetsky, J.B. Bowles, Fourier Analysis of Numerical Approximations of Hyperbolic Equations, SIAM Studies in Applied Mathematics, Philadelphia, 1982.